Tissue and Cell 100 (2026) 103395

Contents lists available at ScienceDirect

Tissue and Cell

journal homepage: www.elsevier.com/locate/tice

# Oxygen-dependent regulation of ADAMTS1 by VEGFA defines a novel VEGFA–HIF–ADAMTS1 axis in hepatocellular cancer

Feray Kockar *, Esra Tokay, Nelin Hacioglu, Kubilay Gunerhan, Yasemin Kalfa, Feyza Nur Sav, Merve Karaman [1], Meltem Balaban, Kubra Zehra Kalay

*Balikesir University, Faculty of Science and Literature, Department of Molecular Biology and Genetics, Balikesir, Turkiye*

ARTICLE INFO

*Keywords:*
ADAMTS1
Hepatocellular cancer
VEGFA
HIF-1α
Angiogenesis

ABSTRACT

ADAMTS1 is a matrix-associated protease involved in angiogenesis and tumor microenvironment remodeling, and its regulation under oxygen-limited conditions has not been fully elucidated. Vascular endothelial growth factor A (VEGFA) is one of the key regulators of angiogenesis and hypoxic signaling. This study aimed to reveal the effects of VEGFA on ADAMTS1 gene expression, promoter activity, and related signaling pathways under normoxic and hypoxic conditions. The findings show that VEGFA regulates ADAMTS1 expression in a time- and oxygen level-dependent manner. Under hypoxic conditions, ADAMTS1 mRNA and protein levels exhibited a biphasic increase, showing a stronger and more persistent response than that under normoxic conditions. Promoter analyses showed that under normoxic conditions, VEGFA suppressed transcriptional activity in both the long (P1) and short (P7) promoter regions, whereas under hypoxic conditions, it decreased P1 activity but induced activation in the P7 region. The partial reversal of this effect by the MEK/ERK inhibitor PD98059 confirmed the role of this pathway in the transcriptional control of VEGFA. Chromatin immunoprecipitation–qPCR further demonstrated oxygen-dependent recruitment of ELK1, c-JUN, and notably ATF-1 to multiple ADAMTS1 promoter regions, with hypoxia inducing a marked and widespread increase in ATF-1 occupancy. Furthermore, it has been determined that VEGFA creates an oxygen-sensitive positive feedback loop by increasing its own expression and HIF-1α stabilization, which in turn enhances ADAMTS1 induction. Integrative bioinformatic analyses of GEO and TCGA-LIHC datasets supported these experimental findings, revealing hypoxia-associated upregulation of VEGFA, positive correlations between hypoxia scores and VEGFA/HIF1A expression, and context-dependent associations between ADAMTS1 expression, hypoxia signaling, and angiogenesis-related gene networks. **T**hese results identify ADAMTS1 as a hypoxia-responsive gene regulated through VEGFA-driven convergence of MAPK and PI3K/AKT signaling on a transcriptionally complex promoter, providing mechanistic insight into hypoxia-associated extracellular matrix remodeling in cancer.

## 1. Introduction

Angiogenesis, the formation of new blood vessels from pre-existing vasculature, is a tightly controlled physiological process that is essential for embryonic development, tissue repair, and wound healing. However, under pathological conditions, angiogenesis contributes to disease progression, including collagen tissue disorders, retinopathies, psoriasis, and particularly tumor growth and metastasis. Malignant tumors can expand only to a volume of approximately 1 $cm^3$ before angiogenesis becomes essential for further proliferation and survival (Lugano et al., 2020). Beyond this critical threshold, neovascularization supplies oxygen and nutrients to the tumor mass, enabling its rapid expansion and invasion into the surrounding tissues. Among the numerous signaling molecules that regulate this process, Vascular

* Correspondence to: Balıkesir University, Faculty of Science and Literature, Department of Molecular Biology and Genetics, Çagis Campus, Balikesïr 10100, Turkiye.

*E-mail addresses:* fkockar@balikesir.edu.tr (F. Kockar), esratokay@balikesir.edu.tr (E. Tokay), nelinhacioglu@balikesir.edu.tr (N. Hacioglu), kubilaygunerhan@gmail.com (K. Gunerhan), yaseminkls06@gmail.com (Y. Kalfa), savnurfeyza@gmail.com (F.N. Sav), mervekaraman@beykent.edu.tr (M. Karaman), balabanmeltem16@gmail.com (M. Balaban), kalayzehra16@gmail.com (K.Z. Kalay).

[1] Present Address: Beykent University Vocational School, Department of Medical Services and Techniques, Program of Medical Laboratory Techniques, 34500 İSTANBUL, TÜRKİYE

https://doi.org/10.1016/j.tice.2026.103395
Received 14 October 2025; Received in revised form 29 January 2026; Accepted 14 February 2026
Available online 16 February 2026

Endothelial Growth Factor A (VEGFA) is the principal driver of angiogenesis. It was initially identified by Senger et al. (1983) as a vascular permeability factor (VPF) that enhances microvascular leakage. VEGFA is now recognized as a potent endothelial cell mitogen (Senger et al., 1983). To date, seven members of the VEGFA gene family have been characterized (Byrne et al., 2005). Elevated VEGFA levels have been observed in multiple malignancies, including cancers of the colon, breast, thyroid, rectum, lung, liver, gallbladder, ovary, and uterus, as well as in angiosarcomas and intracranial tumors (Brogowska et al., 2023). VEGFA is secreted by various cell types, such as smooth muscle cells, fibroblasts, and epithelial cells, and its biological effects are mediated primarily through two tyrosine kinase receptors, VEGFAR1 and VEGFAR2, located on endothelial cells, whereas VEGFAR3 is restricted to the lymphatic endothelium (Ferrara, 2001; Veikkola et al., 2000). Alternative splicing of the VEGFA gene produces several isoforms that regulate capillary morphogenesis and angiogenesis (Fontanini et al., 1997; Srivastava et al., 1988). $VEGFA_{165}$ is one of the most specific mediators of tumor neovascularization. The diffusion capacity of VEGFA isoforms is determined by the heparin-binding domain in the C-terminal region; isoforms lacking this motif, such as $VEGFA_{121}$, diffuse more rapidly through the extracellular matrix (Vempati et al., 2014). Upon ligand binding, VEGFARs dimerize and autophosphorylate, initiating signaling cascades that activate downstream molecules such as PLC-γ, Src, PI3K, and PKC. These signals converge on the Raf–MEK–ERK and PI3K–Akt pathways to promote endothelial cell proliferation, survival, and migration (Hu et al., 2021).

Within this complex network of signaling and extracellular modulation, metalloproteinases play critical roles in tissue remodeling and cell-matrix communication. The ADAM (a disintegrin and metalloproteinase) family consists of zinc-dependent enzymes anchored to the cell membrane and characterized by disintegrin and metalloproteinase domains (Porter et al., 2005; Théret, Bouezzedine, et al., 2021). In 1996, Kuno et al. identified a new family of secreted proteins structurally related to ADAMs but containing thrombospondin type I (TSP1) motifs, which they designated ADAMTS (a disintegrin and metalloproteinase with thrombospondin motifs) (Kuno et al., 1997). Unlike membrane-bound ADAMs, ADAMTS proteins are secreted into the extracellular matrix and combine all ADAM domains with additional TSP repeats that confer unique regulatory properties. The first identified member, ADAMTS1, emerged from a screen for tumor-associated genes expressed in colorectal cancer cells that induced cachexia in mice (Kuno et al., 1997). Subsequent studies have revealed that epigenetic mechanisms play a critical role in its transcriptional regulation. Specifically, promoter hypermethylation reduces ADAMTS1 promoter activity, indicating suppression through DNA methylation (Ahlquist et al., 2008). In parallel, Chou and Chen (2008) demonstrated that treatment with the histone deacetylase inhibitor trichostatin A (TSA) disrupted the binding of SP1 and HDAC6 to the ADAMTS1 promoter, thereby diminishing its transcriptional repression (Chou and Chen, 2008). These findings underscore the fact that ADAMTS1 expression is modulated by chromatin remodeling and histone modification dynamics. In addition to epigenetic control, ADAMTS1 transcription is influenced by hypoxic stress. Hatipoğlu and colleagues (2009) reported that ADAMTS1 mRNA and protein levels markedly increased in endothelial cells exposed to hypoxia, mediated by HIF-1α binding to its promoter region (Hatipoglu et al., 2009). This observation positions ADAMTS1 as an oxygen-sensitive gene intricately linked to the tumor microenvironment (Turkoglu and Kockar, 2016). Indeed, hypoxia defined as oxygen concentrations below 2 %, is a hallmark of the tumor microenvironment (TME) (Altuntaş et al., 2023a). Rapid and uncontrolled tumor proliferation compromises oxygen delivery, particularly in solid tumors such as hepatocellular carcinoma, contributing to poor clinical outcomes. Hypoxia-inducible factors, HIF-1α and HIF-2α, orchestrate a broad adaptive response encompassing metabolic reprogramming, angiogenesis, epithelial–mesenchymal transition (EMT), and therapy resistance (Bakleh and Al Haj Zen, 2025).

Given these insights, ADAMTS1 has attracted considerable attention as a potential tumor angiogenesis suppressor. Tumor invasion and metastasis rely on ECM degradation, in which metalloproteinases, such as ADAMTS enzymes, are pivotal mediators. Reduced ADAMTS1 expression has been reported in hepatocellular carcinoma, pancreatic cancer, and gastrointestinal tumors, while promoter hypermethylation has been associated with its silencing in colorectal, breast, lung, and prostate cancers (Gustavsson et al., 2008; Rocks et al., 2008). Collectively, these findings suggest that ADAMTS1 functions as a negative regulator of angiogenesis and tumor invasion. Mechanistic studies have further revealed that ADAMTS1 directly interacts with pro-angiogenic factors. Vazquez et al. (1999) demonstrated that ADAMTS1 binds VEGFA165 via its two C-terminal TSP repeats, thereby inhibiting both VEGFA- and FGF2-mediated angiogenesis (Luque et al., 2003a; Vázquez et al., 1999). Similarly, Tang (2001) identified a specific GWQRRL/TVECRD motif within the first TSP repeat, shared only with ADAMTS-8, that mediates VEGFA binding (Tang, 2001). These structural and functional relationships highlight ADAMTS1 as an extracellular regulator that counterbalances VEGFA-driven vascularization, maintaining equilibrium in the angiogenic network.

Taken together, accumulating evidence indicates that hypoxia and VEGFA signaling are key regulators of ADAMTS1 transcription and function in tumor-associated angiogenic responses. Accordingly, this study aimed to elucidate the regulatory interplay between VEGFA and ADAMTS1 under normoxic and hypoxic conditions in hepatocellular carcinoma. Using human Hep3B liver carcinoma cells as the primary model, with Saos-2 osteosarcoma cells included to assess tissue-specific responses, we systematically investigated the effects of VEGFA stimulation on ADAMTS1 expression at the mRNA, protein, and promoter levels. Following an initial evaluation of VEGFA-induced cytotoxicity and proliferative responses under both oxygen conditions, time- and dose-dependent analyses were performed to define the dynamic regulation of ADAMTS1. To delineate the intracellular signaling mechanisms involved, pathway inhibition studies targeting MAPK and PI3K/AKT cascades were conducted, and inhibitor efficacy was independently validated by phosphorylation-specific immunoblotting. Promoter-reporter assays employing long and short ADAMTS1 regulatory fragments were used to characterize region-specific transcriptional responses to VEGFA under normoxic and hypoxic conditions, complemented by chromatin immunoprecipitation–qPCR analyses to assess oxygen-dependent recruitment of ELK1, c-JUN, and ATF-1 to the ADAMTS1 promoter. In addition, potential feedback mechanisms were explored by examining VEGFA-induced regulation of VEGFA itself and HIF-1α at both transcript and protein levels. Finally, integrative *in silico* analyses of GEO and TCGA-LIHC datasets were performed to contextualize the experimental findings within a clinically relevant hypoxic tumor environment. This multi-layered approach was designed to provide mechanistic insight into the VEGFA–HIF–ADAMTS1 axis as a hypoxia-sensitive regulatory node in tumor angiogenesis and microenvironment remodeling.

## 2. Materials and methods

### 2.1. *In silico analyses*

Publicly available gene expression data from Hep3B hepatocellular carcinoma cells cultured under normoxic and hypoxic conditions were retrieved from the Gene Expression Omnibus (GEO) database (#GSE271612) and TCGA-LIHC transcriptomic data. Raw count data were normalized using the *DESeq2* package, and differentially expressed genes (DEGs) were identified with an adjusted *p-value* $< 0.05$ and $|\log_2 FC = > 1$. Gene Set Enrichment Analysis (GSEA) was performed using the *clusterProfiler* R package with KEGG and Reactome gene sets to identify pathways enriched in hypoxia-upregulated genes. Single-sample GSEA (ssGSEA) scores for extracellular matrix (ECM) and VEGFA/angiogenesis-related gene signatures were computed using the

*GSVA* package to estimate per-sample pathway activity. Correlation analyses between ADAMTS1, HIF-1α, and VEGFA expression levels were performed using Spearman's rank test, and network visualization of ECM-related gene interactions was generated using *igraph* and *STRINGdb*. The adjusted p-values were calculated using the Benjamini–Hochberg correction.

### 2.2. Cell culture

To passage Hep3B and Saos-2 cells, upon reaching 80–90 % confluence, the culture medium was aspirated. The cells were then washed with sterile phosphate-buffered saline (PBS) and detached using 1 mL of trypsin-ethylenediaminetetraacetic acid (trypsin-EDTA) for 25 $cm^2$ flasks. The cells were then collected using fresh medium, and the pellet was centrifuged at 1000 rpm for 5 min. The cell pellet was dissolved in the medium before seeding into new flasks. The flasks were then labeled and incubated at 37°C with 5 % $CO_2$. The cells were maintained in 25 $cm^2$ flasks, each containing 15 mL of Dulbecco's Modified Eagle Medium (DMEM; Sigma-Aldrich), which was supplemented with 0.2 mM L-Glutamine (Hyclone) and 10 % heat-inactivated (56°C for 1 h) Fetal Calf Serum (Invitrogen). The cultures were passaged biweekly (Alper & Kockar, 2014; Tokay & Kockar, 2016a). To simulate hypoxic conditions, $CoCl_2$ was used at a final concentration of 150 μM (Altuntaş et al., 2023).

### 2.3. Cell proliferation test (MTT Assay)

Before conducting the experiments, 50.000 cells per well were counted using trypan blue and plated into 96-well culture plates. For serum starvation, 0.1 % BSA-containing medium was added to the wells and incubated for 24 h, devoid of serum and cytokines, to facilitate adherence to the surface. Following the incubation period, VEGFA165 was administered at two different concentrations (5 and 20 ng/mL). After 24 h and 48 h incubation time period, MTT solution was added to each well and incubated for 4 h to enable cellular metabolism of MTT. The medium was then removed, and isopropanol containing 0.004 M HCl was added to the wells. After the formazan crystals were dissolved, the absorbance values were measured at 550 nm (Gungor et al., 2018, Güngör et al., 2020, Tokay & Kockar, 2016a).

### 2.4. Transient-transfection and reporter assays

The calcium phosphate precipitation method was used for the transfection assay (Kockar and Yıldırım, 2009). For luciferase assays, Hep3B cells were seeded in 12-well plates at a density of $25 \times 10^4$ cells per well. ADAMTS1 promoter fragments were obtained from Dr. Satoshi Hirohata, Department of Medical Technology, Okayama University (Hatipoglu et al., 2009). The transfection mixture was prepared by adding 1 μg of the ADAMTS1 promoter construct (P1 and P7) and 0.5 μg of the transfection control vector, the secreted human alkaline phosphatase (SEAP) control vector, to control transfection efficiency. pMetLuc control was used as a positive control, and the pMetLuc reporter vector was used as a negative control. After 6 h of transfections, the cells were washed with PBS, and fresh medium was added to the wells. To evaluate the effect of VEGFA on ADAMTS1 transcriptional activity, serum starvation was achieved using 0.1 % BSA 24 h after transfection. The cells were then treated with VEGFA (20 ng/mL) for up to 72 h. Transfection results were obtained using the Ready-To-Glow Secreted Luciferase Reporter System (Clontech). Luciferase activity was normalized to the SEAP values. Each transfection was measured at least three times with Fluoroskan Ascent FL Luminometer (Thermo Electron Co.) (Tokay and Kockar, 2016b).

### 2.5. Real-time PCR

For RNA studies, the GeneJET RNA Purification Kit (Thermo Fisher Scientific) was used to extract total RNA from Hep3B and Saos-2 cells. One microgram of the extracted RNA was converted into complementary DNA (cDNA) using a cDNA synthesis kit (Thermo). qPCR was performed using a Roche instrument, with each set of experiments performed in triplicate. For the amplification of human ADAMTS1, HIF-1α, VEGFA, and human β-2-microglobulin (internal control gene), the primers listed in the supplementary table (Supp. Table 1) was used for each reaction. The Livak method was used to analyze the data (Alper et al., 2025; Livak and Schmittgen, 2001).

### 2.6. Western blotting

RIPA buffer was used to extract proteins from Hep3B cells. Protein concentration was quantified using the Qubit Fluorescent Dye system. Protein samples (30 μg) were mixed with Laemmli buffer and loaded into the wells, and 10 μL of protein size marker (Thermo) was loaded into the first well. The gel was electrophoresed for approximately 90 min by filling the tank (middle and lower sections) with 1X Running Buffer containing 0.1 % (w/v) SDS. The Bio-Rad Trans Blot system (Bio-Rad Laboratories) was used for the electrophoretic transfer of proteins. The cassette was placed into a blot tank filled with transfer buffer, and the transfer was executed at 100 volts for 60 min. The membranes were blocked in 20 mL blocking solution (1X TBS containing 5 % (w/v) non-fat dry milk and 0.1 % (v/v) Tween20) for 1 h at room temperature on a horizontal shaker. The blocking solution was then removed, and the membrane was washed thrice for 5 min each with 1X TBS containing 0.1 % (v/v) Tween20. The membrane was incubated with the primary antibody overnight at room temperature, followed by incubation with the secondary antibody for one hour at room temperature and subsequently imaged. The membranes were treated with ECL (Pierce) substrate for 1–2 min. Images were photographed using the Phusion FX program (Alper and Kockar, 2014; Altuntaş et al., 2023).

### 2.7. IFC method

24-well plates (250,000 / well) were seeded with equal numbers of Hep3B cells. At the same time, round coverslips were placed in these wells. If cytokine treatment was to be applied, it was performed the following day at the designated concentrations. Twenty-four hours after cytokine treatment, the wells were rinsed with PBS. Cells were fixed using 4 % paraformaldehyde. The cells were then permeabilized with PBS containing 0.2 % Triton X100 for 15 min. After washing twice with PBS, 10 % BSA was added to the wells for blocking. Following PBS washing, the cells were incubated overnight at + 4°C in a humidity chamber with primary antibodies (ADAMTS1, VEGFA, and HIF-1α) at a 1/50 dilution. The next day, the primary antibody was removed by washing with PBS. Then, 488 Alexa Fluor (Invitrogen) was applied at a final concentration of 3 μg/mL for 30 min. After washing with PBS, round coverslips were placed on slides using a mounting medium. Images were visualized using fluorescence microscopy and analyzed using ImageJ software (Tokay and Kockar, 2016a).

### 2.8. Pathway studies

Pathway analysis was performed to determine the intracellular signalling pathways activated in Hep3B cells following VEGFA application under normoxic and hypoxic conditions. Hep3B cells were seeded into 6-well plates, incubated overnight at 37°C to ensure cell adhesion, and subjected to 1 h of serum deprivation in medium containing 0.1 % BSA to reduce basal signal activity. Following serum deprivation, cells were pre-incubated with specific pathway inhibitors: the PI3K inhibitor wortmannin (Cell Signaling Technology, #99515; 1 μM), the JNK inhibitor SP600125 (Santa Cruz Biotechnology, sc-200635; 20 μM), and the MAPK/ERK inhibitor PD98059 (Cell Signaling Technology, #9900S; 20 μM) for alternative pathway screening were applied for 45 min. Following inhibitor pre-incubation, 20 ng/mL VEGFA was added to the

cells and incubated for 6 h under normoxic or hypoxic conditions. At the end of the incubation period, cells in parallel sets of experiments were harvested with trypsin/EDTA, centrifuged at 1000 rpm for 5 min, and cell pellets were obtained for qRT-PCR analysis. Under the same experimental conditions, cells were lysed with RIPA buffer for protein extraction, and ADAMTS-1 protein expression levels were analyzed by Western blot. In phosphorylation analyses, PI3 Kinase p85 (19H8) Rabbit mAb (Cell Signaling Technology, #4257), Phospho-PI3 Kinase p85 (Tyr458)/p55 (Tyr199) antibody (Cell Signaling Technology, #4228), SAPK/JNK antibody (Cell Signaling Technology, #9252), and Phospho-SAPK/JNK (Thr183/Tyr185) (81E11) Rabbit mAb (Cell Signaling Technology, #4668) were used (Alper and Kockar, 2014; Castro-Rivera et al., 2008; Chen et al., 2025)

### 2.9. Chromatin immunoprecipitation

The promoter sequence of the ADAMTS1 gene was analysed using the R programming language via the JASPAR 2020 transcription factor binding motif library; potential binding sites for the c-JUN, ATF-1, and ELK-1 transcription factors were identified. A total of 7 ChIP-qPCR primer pairs were designed along the promoter to match these predicted binding sites (Supplementary Table 1). ChIP analyses were performed using the EZ-ChIP™ Chromatin Immunoprecipitation Kit (Millipore, 17–371RF) according to the manufacturer's protocol. Cells were cross-linked with 1 % formaldehyde, chromatin was fragmented into 200–300 bp fragments using sonication, and immunoprecipitation was performed using target protein-specific primer antibodies. For this purpose, anti-c-Jun (Santa Cruz Biotechnology, sc-44), anti-ELK-1 (Santa Cruz Biotechnology, sc-365876) and anti-ATF (Mouse, Santa Cruz Biotechnology, sc-270) antibodies were used; with normal mouse IgG (Santa Cruz Biotechnology, sc-2025) and normal rabbit IgG (Peprotech, 500-P00) applied as negative controls. Antibody–protein–DNA complexes were precipitated with protein G agarose beads, eluted after washing steps, and cross-links were cleaved. Purified DNA samples were analysed by qRT-PCR; ChIP enrichment was calculated by subtracting the average IgG Ct value from the target ChIP Ct

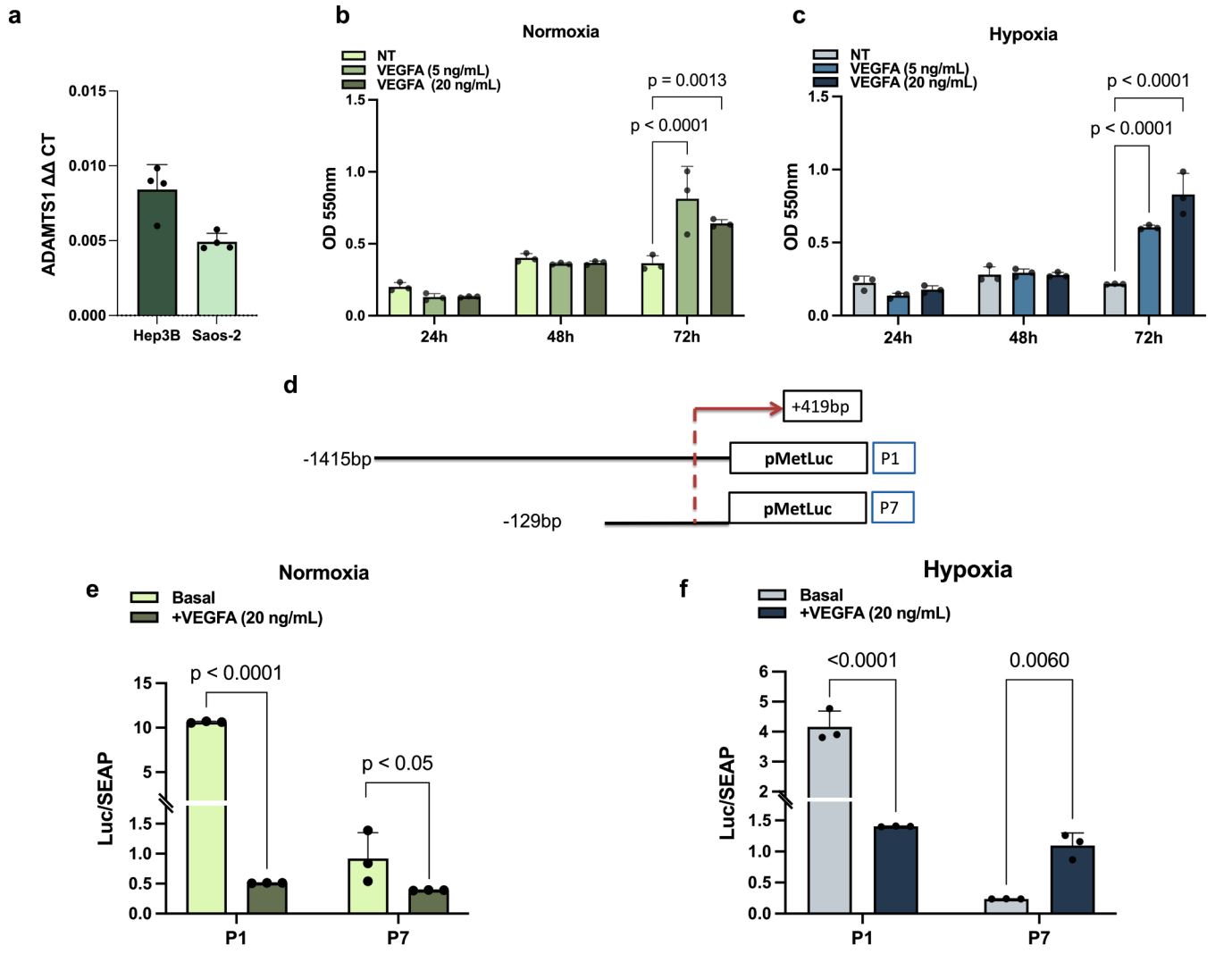


**Fig. 1.** Effects of VEGFA on ADAMTS1 expression and promoter activity.(a) Basal ADAMTS1 mRNA expression levels in Hep3B and Saos-2 cells determined by quantitative RT-PCR and expressed as ΔCt values. (b–c) Time-dependent effects of VEGFA stimulation on cellular metabolic activity under normoxic (b) and hypoxic (c) conditions. Cells were treated with VEGFA (5 or 20 ng/mL) for 24, 48, and 72 h, and cell viability was assessed by MTT assay (OD 550 nm). Exact p values are indicated. (d) Schematic representation of the human ADAMTS1 promoter constructs used in luciferase reporter assays. The full-length promoter fragment (P1; −1415 to +419 bp) and the truncated proximal promoter fragment (P7; −129 to +419 bp) were cloned upstream of the secreted alkaline phosphatase (SEAP) reporter gene in the pMetLuc vector. (e–f) ADAMTS1 promoter activity under normoxic (e) and hypoxic (f) conditions in cells transfected with P1 or P7 constructs and treated with VEGFA (20 ng/mL). Promoter activity was measured as Luc/SEAP ratios. Individual data points represent biological replicates, and bars indicate mean ± SD. Exact p values are shown. All experiments were performed with n = 3 independent biological replicates.

values (ΔCt), and fold enrichment values were determined using the 2^ (–ΔCt) method (Alper et al., 2025; Nelson, 2006).

### 2.10. Statistical analysis

All statistical analyses were performed using the GraphPad Prism software (GraphPad Software, San Diego, CA, USA). Statistical significance was set at $p < 0.05$. One-way ANOVA was used for experiments with a single independent variable, and two-way ANOVA was used for experiments with two independent variables. The stars in the figures indicate the following levels of significance: *$p < 0.05$ (*), $p < 0.01$ (**), $p < 0.001$ (***), and $p < 0.0001$ (****).*

## 3. Results

### 3.1. The effects of VEGFA application on ADAMTS1 expression and promoter activity

The basal expression levels of ADAMTS1 mRNA were analyzed in Hep3B and Saos-2 cell lines using quantitative real-time PCR. As shown in the graph (Fig. 1a), Hep3B cells exhibited higher ADAMTS1 transcript levels than Saos-2 cells, although the difference was not statistically significant ($p > 0.05$). This trend indicates that ADAMTS1 may be more actively transcribed in liver-derived cells, suggesting a tissue-specific regulatory pattern. These findings provide a reference for subsequent experiments evaluating how VEGFA stimulation and hypoxic stress modulate ADAMTS1 transcriptional activity in different cellular contexts.

VEGFA is a key regulator of angiogenesis and cellular adaptation under conditions of oxygen imbalance. Therefore, examining the effects of different VEGFA doses on cell proliferation under normoxic and

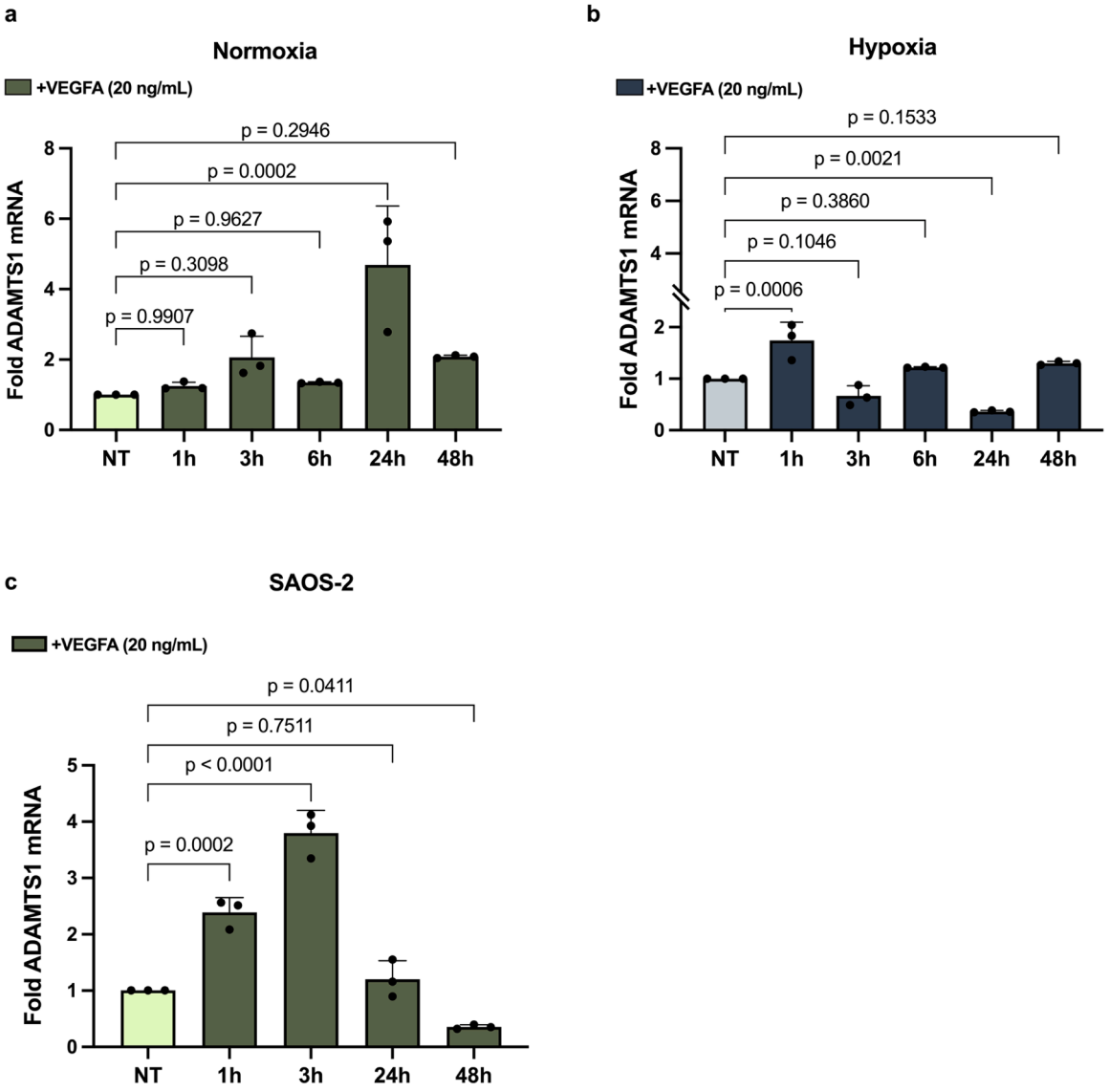


**Fig. 2.** Time-dependent ADAMTS1 mRNA response to VEGFA under normoxic and hypoxic conditions (a–b) Time-course analysis of ADAMTS1 mRNA expression in response to VEGFA (20 ng/mL) treatment under normoxic (a) and hypoxic (b) conditions. Cells were treated with VEGFA for the indicated time points, and ADAMTS1 mRNA levels were quantified by quantitative RT-PCR and expressed as fold change relative to non-treated (NT) controls. (c) Time-dependent ADAMTS1 mRNA expression in SAOS-2 cells following VEGFA (20 ng/mL) treatment under normoxic conditions. Individual data points represent biological replicates, and bars indicate mean ± SD. Exact p values are shown. All experiments were performed with n = 3 independent biological replicates.

hypoxic conditions is critical for elucidating the functional importance of hypoxia response mechanisms and VEGFA-mediated signaling pathways. The effects of VEGFA on cell proliferation were evaluated at 24, 48, and 72 h under normoxic and hypoxic conditions using two different doses (5 and 20 ng/mL). Under normoxic conditions (Fig. 1b), VEGFA administration, particularly at high doses, led to a significant increase in cell proliferation at 72 h ($p < 0.01$, $p < 0.0001$). Under low oxygen conditions (Fig. 1c), the proliferative effect was more pronounced at the same time point; 20 ng/mL VEGFA application significantly increased cell growth compared to the 5 ng/mL dose ($p < 0.0001$).

To evaluate the effect of VEGFA on ADAMTS1 promoter activity, constructs containing long (P1: −1415/+419) and short (P7: −129/+419 bp) promoter fragments were analyzed under normoxic and hypoxic conditions, respectively (Fig. 1d). Under normoxic conditions (Fig. 1e), VEGFA application caused a significant decrease in P1 promoter activity compared to the basal activity ($p < 0.0001$), suggesting that VEGFA exerts a transcriptional inhibitory effect on the long-promoter region. Similarly, a significant decrease was observed in the P7 promoter after VEGFA application ($p < 0.05$). Under hypoxic conditions (Fig. 1f), VEGFA application significantly reduced the basal activity in the P1 fragment ($p < 0.01$), whereas there was an upregulatory effect of VEGFA on the transcriptional activity of the P7 fragment. These findings reveal that the effect of VEGFA may vary depending on oxygen levels.

### 3.2. *VEGFA induces ADAMTS1 expression in a time- and oxygen-dependent manner*

Quantitative RT-PCR analyses further confirmed the oxygen-dependent regulation of ADAMTS1 at mRNA level (Fig. 2a-b). In normoxic Hep3B cells, VEGFA treatment resulted in a significant, time-dependent increase in ADAMTS1 mRNA expression, with the highest induction observed at 24 h (approximately 4.2-fold compared with the non-treated control; $p < 0.0001$) (Fig. 2a). In contrast, under hypoxia, ADAMTS1 mRNA expression followed a biphasic pattern, characterized by an early transient increase at 6 h ($p < 0.0001$), followed by a second peak at 48 h ($p < 0.01$). These results indicate that VEGFA exerts distinct temporal mRNA expression effects on ADAMTS1, depending on oxygen availability.

In analyses comparing the response to VEGF administration in Saos-2 and Hep3B cells, the time-dependent expression change of ADAMTS1 was evaluated. VEGF administration caused a significant increase in ADAMTS1 mRNA levels during the early period. This increase, which began particularly at 1 h, peaked at 3 h, showing an approximately four-fold increase ($p < 0.0001$). However, this increase was transient, and ADAMTS1 expression approached basal levels at 24 and 48 h. This dynamic expression pattern indicates that VEGF transiently activates ADAMTS1 transcription in Saos-2 cells, suggesting that this gene may play a role in VEGF-mediated early cellular response mechanisms (Fig. 2c).

To determine whether VEGFA influences ADAMTS1 expression in hepatocellular carcinoma cells, Hep3B cells were stimulated with recombinant VEGFA (20 ng/mL) under normoxic and hypoxic conditions. Immunofluorescence analysis revealed a marked increase in ADAMTS1 signal intensity following VEGFA treatment under both conditions (Fig. 3a). Under normoxia, VEGFA stimulation led to a nearly two-fold increase ($p < 0.001$) in corrected total cell fluorescence (CTCF) compared to untreated controls, whereas under hypoxia, ADAMTS1 fluorescence increased by approximately three-fold ($p < 0.0001$), indicating a more pronounced response in oxygen-limited environments than in normoxic environments. These results suggest that VEGFA upregulates ADAMTS1 expression at the cellular level, and this effect is

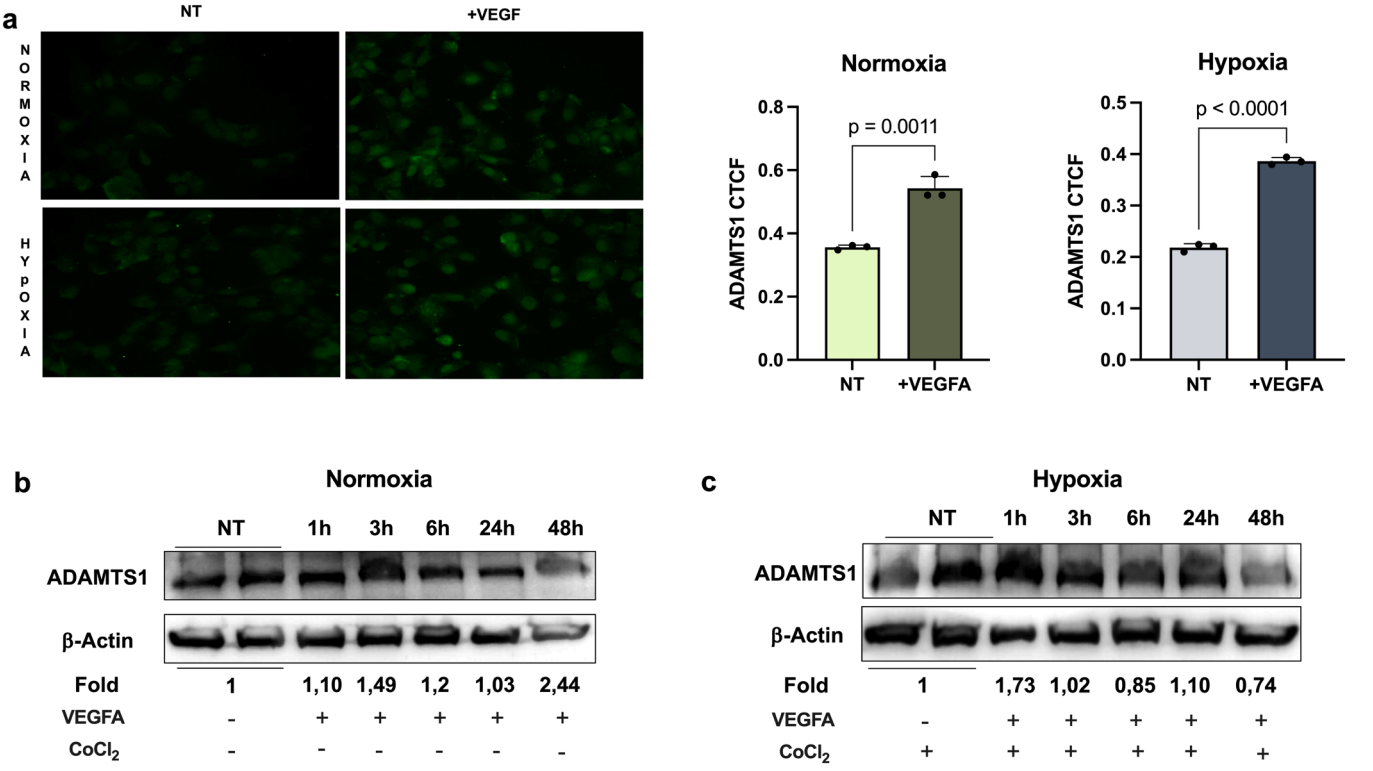


**Fig. 3.** ADAMTS1 protein expression following VEGFA treatment under normoxic and hypoxic conditions (a) Representative immunofluorescence images showing ADAMTS1 protein expression in Hep3B cells cultured under normoxic and hypoxic conditions in the presence or absence of VEGFA (20 ng/mL). ADAMTS1 immunoreactivity is shown in green. Quantification of corrected total cell fluorescence (CTCF) is shown on the right. Bars represent mean ± SD from n = 3 independent biological replicates. Exact p values are indicated. (b–c) Representative Western blot images showing ADAMTS1 protein levels following VEGFA (20 ng/mL) treatment at the indicated time points (1–48 h) under normoxic (b) and hypoxic (c) conditions. β-actin was used as a loading control. Numbers below the blots indicate densitometric fold changes relative to non-treated (NT) controls after normalization to β-actin.

augmented by hypoxic stress.

Western blot analysis corroborated the immunofluorescence data, demonstrating the dynamic regulation of ADAMTS1 protein levels over time following VEGFA stimulation (Fig. 3b-c). Under normoxia, ADAMTS1 expression progressively increased, peaking at 48 h (2.4-fold relative to control) (Fig. 2b), whereas under hypoxia, protein levels transiently rose at 1 h (1.7-fold) but subsequently declined after 6 h, returning to baseline by 48 h (Fig. 3c). These results indicate that hypoxia alters the temporal kinetics of ADAMTS1 induction by VEGFA, suggesting rapid but transient activation of the protein under low-oxygen conditions.

### 3.3. Pathway-associated and transcription factor–linked modulation of ADAMTS1 under normoxic and hypoxic conditions

To investigate whether the effect of VEGFA on ADAMTS1 promoter activity is regulated via the MEK/ERK signaling pathway, the PD98059 (PD9) inhibitor, which specifically suppresses this pathway, was used in the experiments. In this study, two different promoter regions representing the transcriptional activity of the ADAMTS1 gene were evaluated under normoxic and hypoxic conditions. Under normoxic conditions (Fig. 4a), VEGFA application caused a significant decrease in both P1 ($p < 0.0001$) and P7 ($p < 0.05$) promoter fragments compared to the basal activity. The addition of the MEK inhibitor PD9 did not eliminate this inhibitory effect; rather, it maintained low levels of transcriptional activity. Under hypoxic conditions (Fig. 4b), VEGFA application reduced activity in the P1 promoter ($p < 0.05$) but caused a marked activation in the P7 fragment ($p < 0.01$). This indicates that VEGFA exerts a region-specific regulatory effect on ADAMTS1 promoter regions and that the short promoter fragment is sensitive to VEGFA-mediated transcriptional activation under hypoxic conditions. Co-treatment with the MEK/ERK pathway inhibitor PD98059 markedly attenuated VEGFA-induced luciferase activity, particularly in the proximal promoter construct (P7), confirming that ERK signaling contributes to VEGFA-induced transcriptional activation of ADAMTS1.

To further investigate transcription factor involvement, *in silico* promoter analysis identified multiple putative binding sites for ELK1, c-JUN, and ATF-1 within the ADAMTS1 promoter region. Chromatin immunoprecipitation (ChIP–qPCR) assays were then performed to assess transcription factor occupancy at selected promoter regions under normoxic and hypoxic conditions. Under normoxia, ELK1 occupancy was detected at specific ADAMTS1 promoter regions relative to IgG controls (Fig. 4c). Under hypoxia, ELK1 enrichment was observed at distinct promoter sites, suggesting oxygen-sensitive differences in promoter association (Fig. 4d). ChIP–qPCR analyses further revealed detectable binding of c-JUN to the ADAMTS1 promoter under both normoxic and hypoxic conditions, with differential enrichment patterns across promoter regions (Fig. 4e–f). As shown in Figure **g**, ATF-1 binding under normoxia was detectable but largely restricted, with modest enrichment observed at selected regions compared to the IgG control. In particular, significant enrichment was detected at ChIP6 and ChIP7 regions ($p < 0.0001$), indicating basal ATF-1 occupancy under normoxic conditions.

In contrast, exposure to hypoxia resulted in a marked and widespread increase in ATF-1 binding across multiple predicted ATF-1 response elements (Fig. 4h). Under hypoxic conditions, ATF-1 exhibited significantly higher enrichment at nearly all examined ChIP regions compared with IgG controls ($p < 0.0001$), with several loci showing substantially elevated fold enrichment relative to normoxia. Notably, regions corresponding to ChIP1–ChIP6 displayed robust ATF-1 occupancy, indicating a hypoxia-dependent enhancement of ATF-1 recruitment to these genomic sites. These findings indicate that multiple transcription factors associated with MAPK- and stress-responsive signaling pathways can associate with the ADAMTS1 promoter in an oxygen-dependent manner.

To validate that the pharmacological inhibitors used in this study effectively blocked their respective signaling pathways, pathway-specific phosphorylation states were examined by western blot analysis under the same experimental conditions used for ADAMTS1 regulation assays. Cells were serum-starved with BSA for 1 h, pretreated with the indicated inhibitors for 45 min, and subsequently stimulated with VEGFA. Hypoxic conditions were established using $CoCl_2$-mediated chemical hypoxia, while parallel experiments were performed under normoxia.As shown in Supplementary Figure S1, VEGFA stimulation under normoxic conditions resulted in a clear induction of PI3K phosphorylation, which was efficiently suppressed by wortmannin treatment, confirming effective inhibition of the PI3K/AKT pathway (Supplementary Figure S1). Total PI3K and β-actin levels remained unchanged, indicating pathway-specific inhibition rather than global protein loss. Similarly, under $CoCl_2$-induced hypoxic conditions, VEGFA robustly increased SAPK/JNK phosphorylation, whereas pretreatment with th e JNK inhibitor SP600125 markedly reduced p-SAPK/JNK levels without affecting total protein expression (Supplementary Figure S1). These findings confirm that the applied inhibitors effectively blocked their intended signaling cascades under both normoxic and hypoxic conditions.

Finally, the effects of pathway inhibition on ADAMTS1 protein levels were examined by western blot analysis. Western blot analysis demonstrated that VEGFA increased ADAMTS1 protein expression under both normoxic and hypoxic conditions (Fig. 4i–j). Inhibitor treatments revealed that PD169316 (p38/MAPK), PD98059 (MEK/ERK), SP600125 (JNK), and wortmannin (PI3K/AKT) markedly reduced VEGFA-induced ADAMTS1 expression under both hypoxic and normoxic conditions. SP600125 (JNK) exerted a moderate suppressive effect under hypoxic conditions, suggesting a context-dependent contribution of JNK signaling. In contrast, wortmannin (PI3K/AKT) showed a more pronounced inhibitory effect under normoxic conditions. These data demonstrate that the observed reduction in ADAMTS1 expression following inhibitor treatment reflects bona fide pathway inhibition, as independently validated by phosphorylation-specific analyses. Collectively, these findings indicate that VEGFA-induced ADAMTS1 expression requires the coordinated activation of p38/MAPK, MEK/ERK, JNK, and PI3K/AKT signaling pathways under both normoxic and hypoxic conditions (Fig. 4i–j).

### 3.4. Evidence supporting oxygen-dependent VEGFA autoregulation

To investigate whether VEGFA expression is associated with hypoxic conditions in liver cancer, publicly available transcriptomic data derived from liver cancer patients were analyzed using a GEO dataset. As shown in Fig. 5**a**, VEGFA expression levels were compared between normoxic and hypoxic sample groups. Quantitative analysis revealed that VEGFA expression was markedly higher in hypoxic tumor samples compared with normoxic counterparts. While VEGFA expression under normoxia was detected at moderate levels, hypoxic samples exhibited a clear upward shift in expression distribution, with higher median and upper quartile values. Statistical analysis demonstrated a trend toward increased VEGFA expression in hypoxic conditions ($p = 1e{-}01$), indicating an association between hypoxia and elevated VEGFA transcription in liver cancer tissues. To further validate the association between hypoxia and VEGFA expression in liver cancer, transcriptomic data from the TCGA-LIHC cohort were analyzed. A hypoxia score was calculated for each tumor sample using a predefined hypoxia gene signature, explicitly excluding VEGFA from the scoring algorithm to avoid circular bias. VEGFA expression levels were then correlated with the resulting hypoxia scores. As shown in Fig. 5**b**, VEGFA expression exhibited a positive correlation with hypoxia scores across TCGA-LIHC tumor samples (Spearman's $\rho = 0.16$, $p = 0.0098$; $n = 423$). Density contour visualization revealed a gradual rightward shift toward higher VEGFA expression values with increasing hypoxia scores, indicating that tumors characterized by a more hypoxic transcriptional profile tend to express higher levels of VEGFA.

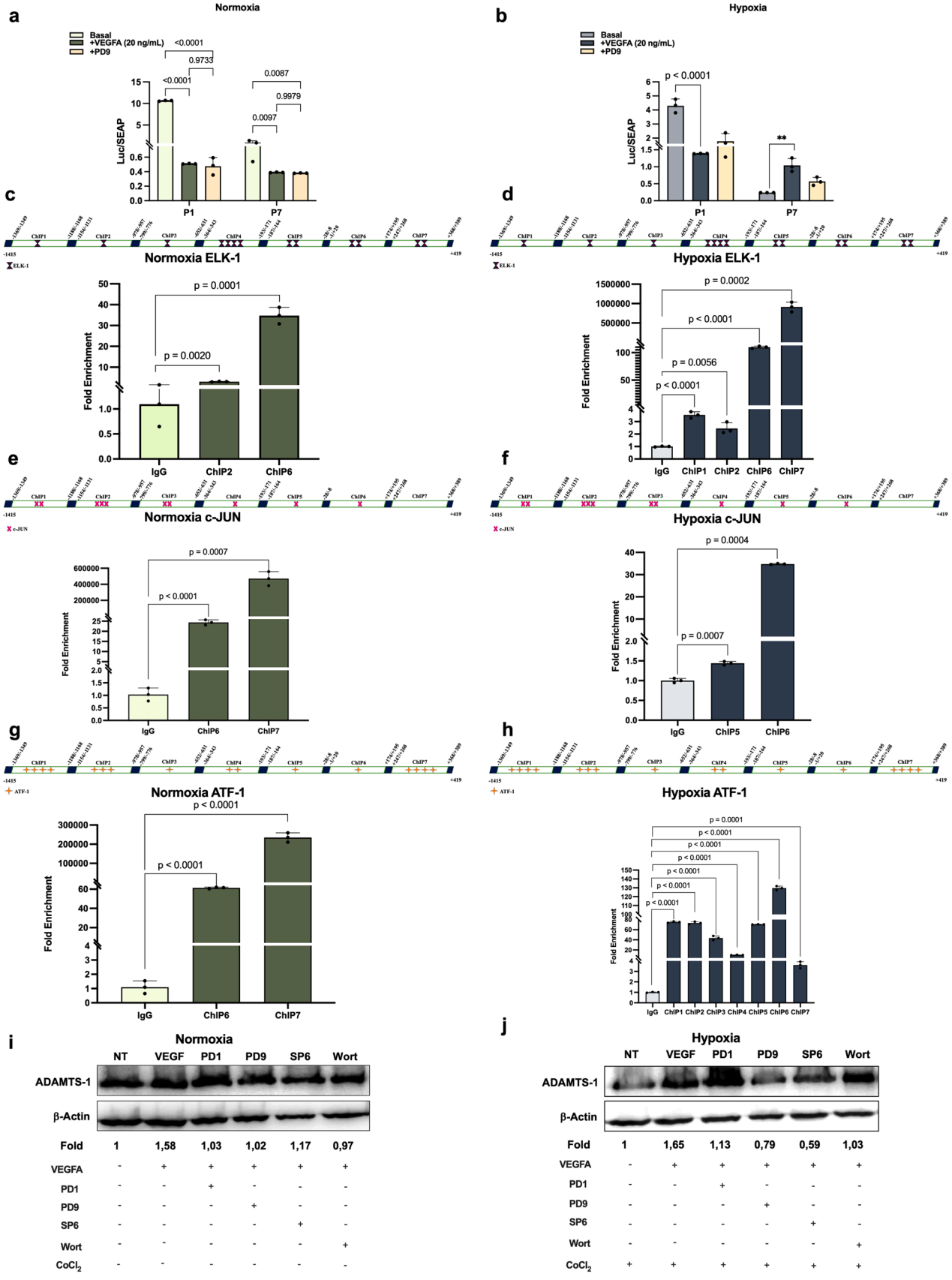


*(caption on next page)*

**Fig. 4.** Transcription factor binding at the ADAMTS1 promoter and pathway-associated changes in ADAMTS1 expression under normoxia and hypoxia (a–b) ADAMTS1 promoter activity under normoxic (a) and hypoxic (b) conditions following VEGFA (20 ng/mL) stimulation in the presence or absence of pharmacological pathway inhibitors. Cells were transfected with ADAMTS1 promoter constructs and promoter activity was assessed using Luc/SEAP reporter assays. Basal, VEGFA-treated, and inhibitor-treated conditions are shown. Exact p values are indicated. (c–d) Schematic representation of predicted transcription factor binding sites within the ADAMTS1 promoter region and chromatin immunoprecipitation (ChIP–qPCR) analysis of ELK1 occupancy at selected promoter regions under normoxic (c) and hypoxic (d) conditions. Enrichment is expressed as fold change relative to IgG controls. (e–f) ChIP–qPCR analysis of c-JUN binding to the ADAMTS1 promoter under normoxic (e) and hypoxic (f) conditions. Enrichment values are shown relative to IgG controls. (g–h) ChIP–qPCR analysis of ATF-1 occupancy at the ADAMTS1 promoter under normoxic (g) and hypoxic (h) conditions. Enrichment is expressed as fold change relative to IgG. (i–j) Representative Western blot images showing ADAMTS1 protein levels following VEGFA stimulation in the presence or absence of pathway inhibitors under normoxic (i) and hypoxic (j) conditions. β-actin was used as a loading control. Numbers below the blots indicate densitometric fold changes relative to non-treated (NT) controls after normalization to β-actin. For ChIP–qPCR and luciferase assays, bars represent mean ± SD from n = 3 independent biological replicates. Exact p values are shown. Western blot images are representative of the experimental conditions shown.

Although the correlation strength was modest, the association was statistically significant, consistent with the multifactorial regulation of VEGFA in heterogeneous tumor tissues. These findings support a clinically relevant link between hypoxic tumor microenvironments and VEGFA expression in hepatocellular carcinoma and complement the experimental data demonstrating hypoxia-dependent VEGFA signaling in endothelial cells. These patient-derived data support a clinically relevant link between hypoxic tumor microenvironments and increased VEGFA expression in liver cancer and provide translational context for the *in vitro* findings presented in this study.

To examine whether VEGFA expression is responsive to exogenous VEGFA stimulation under different oxygen conditions, Hep3B cells were treated with recombinant VEGFA (20 ng/mL), and VEGFA expression was assessed at both transcript and protein levels (Fig. 5c–i). Immunofluorescence analysis demonstrated increased VEGFA protein signal intensity following VEGFA treatment under both normoxic and hypoxic conditions, with a more pronounced response observed under hypoxia (Fig. 5c). Quantification of corrected total cell fluorescence (CTCF) confirmed that VEGFA-associated induction of VEGFA protein levels was enhanced under reduced oxygen tension (Fig. 5d–e). Time-course analysis using quantitative RT-PCR revealed that VEGFA stimulation was associated with increased VEGFA mRNA expression under both oxygen conditions. Under normoxia, VEGFA transcript levels increased progressively and remained elevated over time (Fig. 5f). In contrast, under hypoxic conditions, VEGFA mRNA levels increased more rapidly and reached higher maximal levels, followed by a sustained plateau phase (Fig. 5g). Consistent with transcript-level observations, western blot analysis showed a gradual increase in VEGFA protein abundance following VEGFA treatment under both normoxic and hypoxic conditions, with a stronger and more sustained response detected under hypoxia (Fig. 5h–i).

### 3.5. Association between VEGFA stimulation and HIF-1α expression under normoxic and hypoxic conditions

To assess whether VEGFA stimulation is associated with changes in HIF-1α expression under different oxygen conditions, Hep3B cells were treated with recombinant VEGFA (20 ng/mL) and HIF-1α levels were analyzed at both the transcript and protein levels (Fig. 6a–g). Immunofluorescence analysis revealed that VEGFA treatment was associated with increased nuclear HIF-1α signal intensity under normoxic conditions (Fig. 6a–b). Quantitative CTCF analysis confirmed a significant increase in HIF-1α fluorescence following VEGFA stimulation compared to non-treated controls (Fig. 6b). Under hypoxic conditions, HIF-1α signal intensity was markedly elevated, and VEGFA treatment was associated with a further increase in nuclear HIF-1α accumulation (Fig. 6a and c), indicating enhanced responsiveness of HIF-1α protein levels in a low-oxygen environment. Time-course analysis by quantitative RT-PCR demonstrated that VEGFA stimulation was associated with increased HIF-1α mRNA expression under both oxygen conditions (Fig. 6d–e). Under normoxia, a moderate but sustained induction of HIF-1α transcripts was observed over time, whereas under hypoxia, transcript levels increased more rapidly and reached substantially higher levels, remaining elevated throughout the analyzed time points. Consistent with transcript-level findings, western blot analysis showed time-dependent changes in HIF-1α protein abundance following VEGFA treatment under both normoxic and hypoxic conditions (Fig. 6f–g). Under normoxia, HIF-1α protein levels exhibited transient increases at early and late time points, whereas under hypoxia, VEGFA treatment was associated with a stronger and more sustained accumulation of HIF-1α protein.

### 3.6. Hypoxia-associated transcriptional relationships among VEGFA, HIF-1α, and ADAMTS1 in TCGA-LIHC

To investigate whether the oxygen-dependent relationships observed *in vitro* are reflected at the transcriptomic level in human tumors, we performed comprehensive bioinformatic analyses using RNA-sequencing data from the TCGA-LIHC cohort (Fig. 7a–k). This analysis aimed to contextualize the experimental findings within a clinically relevant hypoxic tumor environment. Kaplan–Meier overall survival analysis stratified by ADAMTS1 expression (median split) did not reveal a statistically significant difference between high and low expression groups (Fig. 7a), indicating that ADAMTS1 expression alone is not sufficient to predict patient outcome in hepatocellular carcinoma. This finding suggests that the biological role of ADAMTS1 may be context-dependent rather than prognostic in isolation. Comparative expression analysis between tumor and normal liver tissues demonstrated altered expression patterns of both VEGFA and ADAMTS1 in TCGA-LIHC samples (Fig. 7b–c), consistent with tumor-associated remodeling of angiogenic and extracellular matrix–related pathways. To further explore hypoxia-associated expression dynamics, hypoxia scores were calculated and correlated with gene expression levels across the cohort. ADAMTS1 expression exhibited a non-linear relationship with hypoxia score (Fig. 7d), suggesting that its expression may be modulated differently across varying hypoxic states within tumors. Importantly, this association persisted when the hypoxia score was recalculated excluding VEGFA expression to avoid potential circularity (Fig. 7e), supporting the robustness of the observed relationship. Stratification of samples based on hypoxia status further revealed a hypoxia-dependent association between ADAMTS1 and VEGFA expression, with distinct correlation patterns observed in low- and high-hypoxia groups (Fig. 7f). These findings indicate that the relationship between ADAMTS1 and VEGFA is influenced by the hypoxic context rather than representing a uniform correlation across all samples.

Consistent with its established role in hypoxic signaling, VEGFA expression showed a positive correlation with hypoxia score when VEGFA was excluded from the hypoxia signature (Fig. 7g). In parallel, HIF1A expression also displayed a positive association with hypoxia score (Fig. 7h), supporting the validity of the hypoxia scoring approach and reinforcing the relevance of HIF-1α–mediated transcriptional responses in this cohort. To gain further insight into the biological processes associated with ADAMTS1 expression, gene co-expression analysis was performed using ADAMTS1 as a reference. Gene Ontology (GO) biological process enrichment analysis of ADAMTS1 co-expressed genes revealed significant enrichment of pathways related to

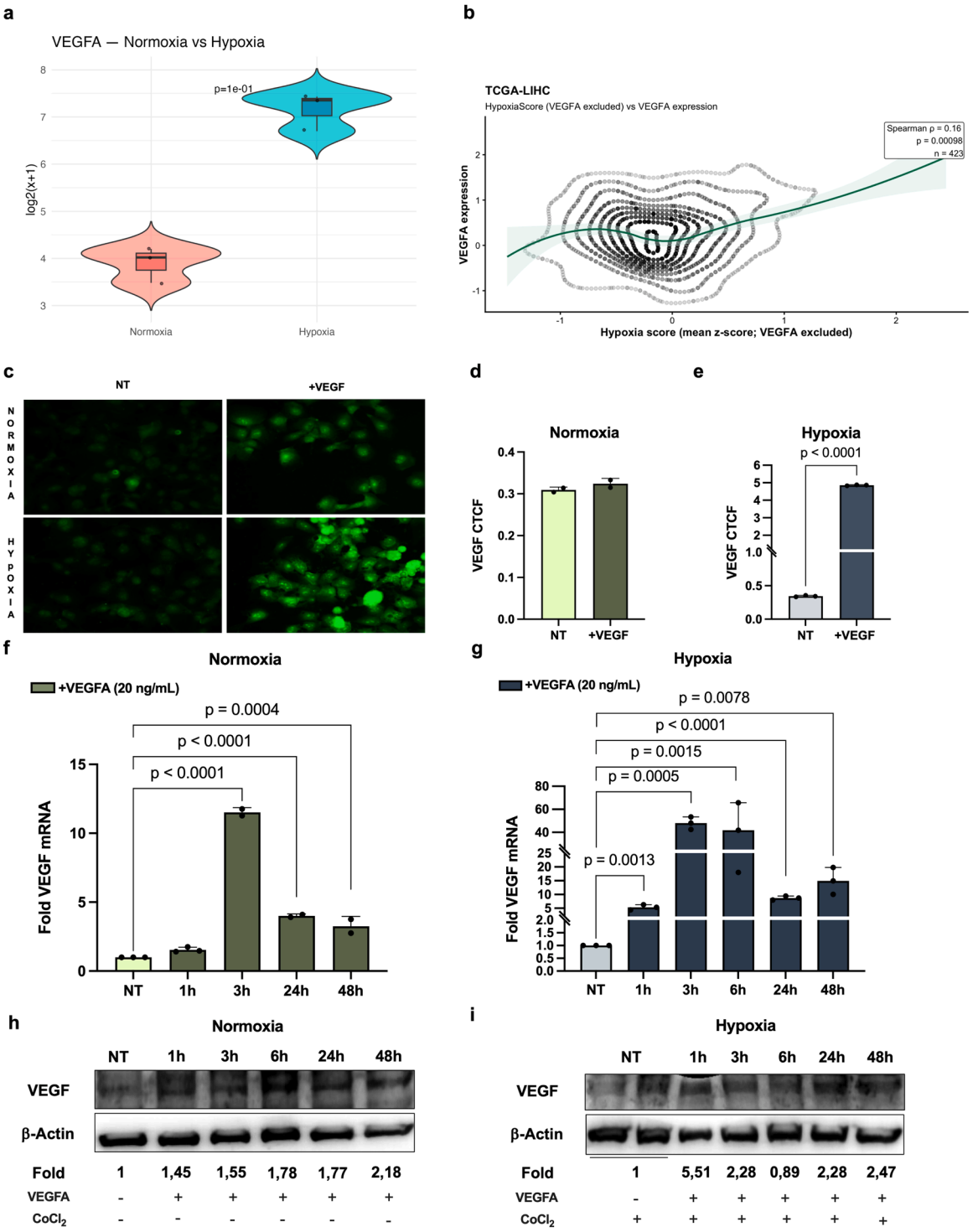


**Fig. 5.** Evidence supporting an oxygen-dependent VEGFA autoregulatory loop in experimental models (a) Comparison of VEGFA expression levels under normoxic and hypoxic conditions shown as violin plots. Expression values are presented as log2-transformed data. (b) Correlation analysis between VEGFA expression and hypoxia score in the TCGA-LIHC cohort. The hypoxia score was calculated excluding VEGFA expression to avoid circularity. Spearman correlation coefficient (ρ), p value, and sample size (n) are indicated. (c) Representative immunofluorescence images showing VEGFA protein expression in cells cultured under normoxic and hypoxic conditions in the presence or absence of recombinant VEGFA (20 ng/mL). VEGFA immunoreactivity is shown in green. (d–e) Quantification of corrected total cell fluorescence (CTCF) for VEGFA under normoxic (d) and hypoxic (e) conditions. (f–g) Time-dependent VEGFA mRNA expression following recombinant VEGFA (20 ng/mL) treatment under normoxic (f) and hypoxic (g) conditions, assessed by quantitative RT-PCR and expressed as fold change relative to non-treated (NT) controls. (h–i) Representative Western blot images showing VEGFA protein levels at the indicated time points (1–48 h) under normoxic (h) and hypoxic (i) conditions. β-actin was used as a loading control. Numbers below the blots indicate densitometric fold changes relative to non-treated (NT) controls after normalization to β-actin. For immunofluorescence quantification and qRT-PCR analyses, bars represent mean ± SD from n = 3 independent biological replicates. Western blot images are representative of the experimental conditions shown.

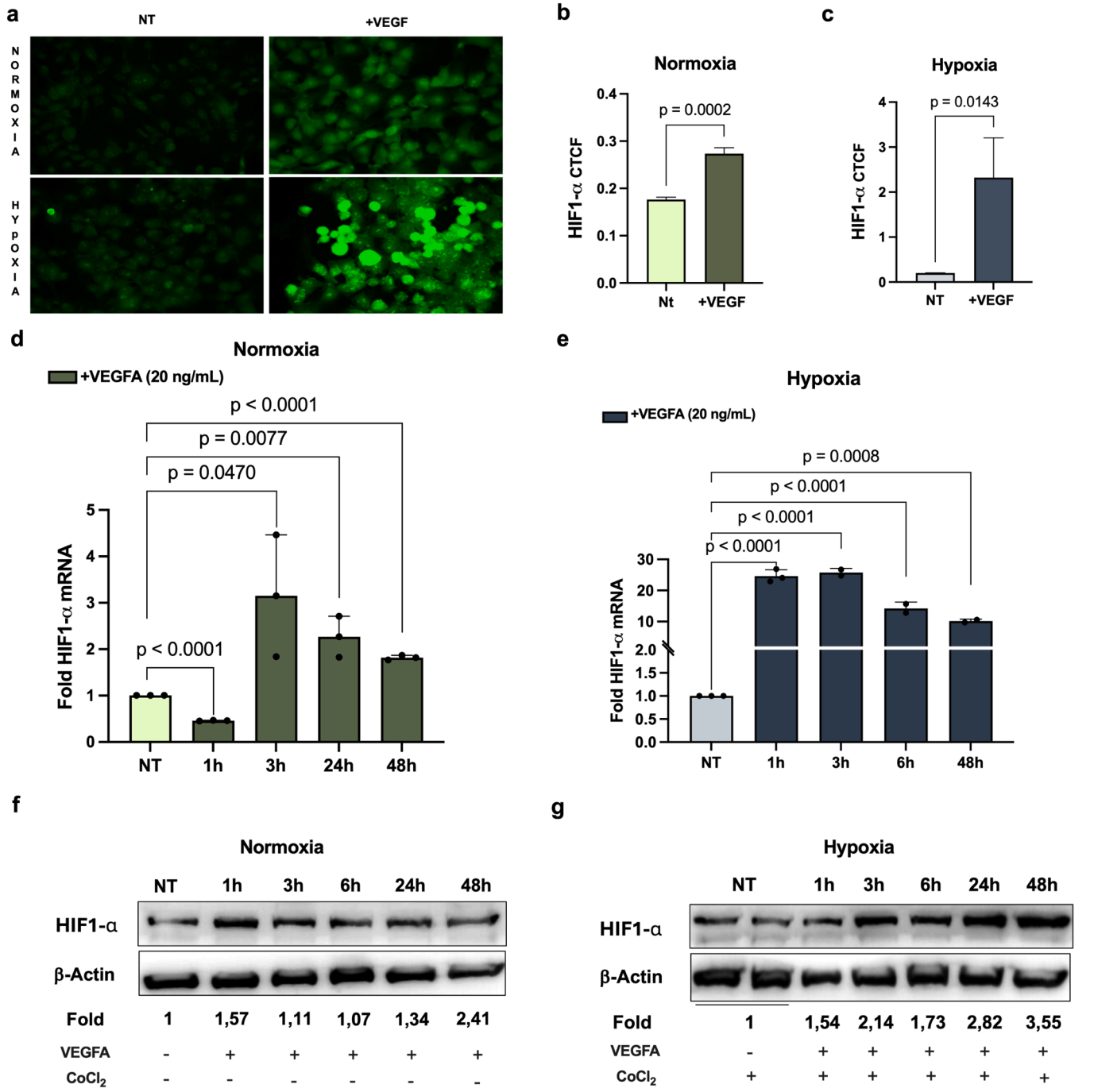


**Fig. 6.** Association between VEGFA stimulation and HIF-1α expression under normoxic and hypoxic conditions (a) Representative immunofluorescence images showing HIF-1α protein expression in Hep3B cells cultured under normoxic and hypoxic ($CoCl_2$) conditions in the presence or absence of recombinant VEGFA (20 ng/mL). HIF-1α immunoreactivity is shown in green. (b–c) Quantification of corrected total cell fluorescence (CTCF) for HIF-1α under normoxic (b) and hypoxic (c) conditions. (d–e) Time-dependent HIF-1α mRNA expression following VEGFA (20 ng/mL) treatment under normoxic (d) and hypoxic (e) conditions, assessed by quantitative RT-PCR and expressed as fold change relative to non-treated (NT) controls. (f–g) Representative Western blot images showing HIF-1α protein levels at the indicated time points (1–48 h) following VEGFA treatment under normoxic (f) and hypoxic (g) conditions. β-actin was used as a loading control. Numbers below the blots indicate densitometric fold changes relative to NT controls after normalization to β-actin. For immunofluorescence quantification and qRT-PCR analyses, bars represent mean ± SD from n = 3 independent biological replicates. Western blot images are representative of the experimental conditions shown.

extracellular matrix organization, vascular development, angiogenesis, and regulation of endothelial cell function (Fig. 7i). These processes are consistent with known roles of ADAMTS family members in tumor microenvironment remodeling.

Network analysis of the top ADAMTS1 co-expressed genes highlighted interconnected gene clusters enriched for hypoxia-responsive and angiogenesis-related signaling pathways (Fig. 7j), further supporting the integration of ADAMTS1 within hypoxia-associated transcriptional programs. In addition, KEGG pathway enrichment analysis identified multiple hypoxia- and stress-related signaling pathways among genes upregulated under hypoxic conditions, including HIF-1 signaling, MAPK signaling, and angiogenesis-associated pathways (Fig. 7k). Collectively, these *in silico* analyses extend the experimental observations by demonstrating that VEGFA, HIF-1α, and ADAMTS1

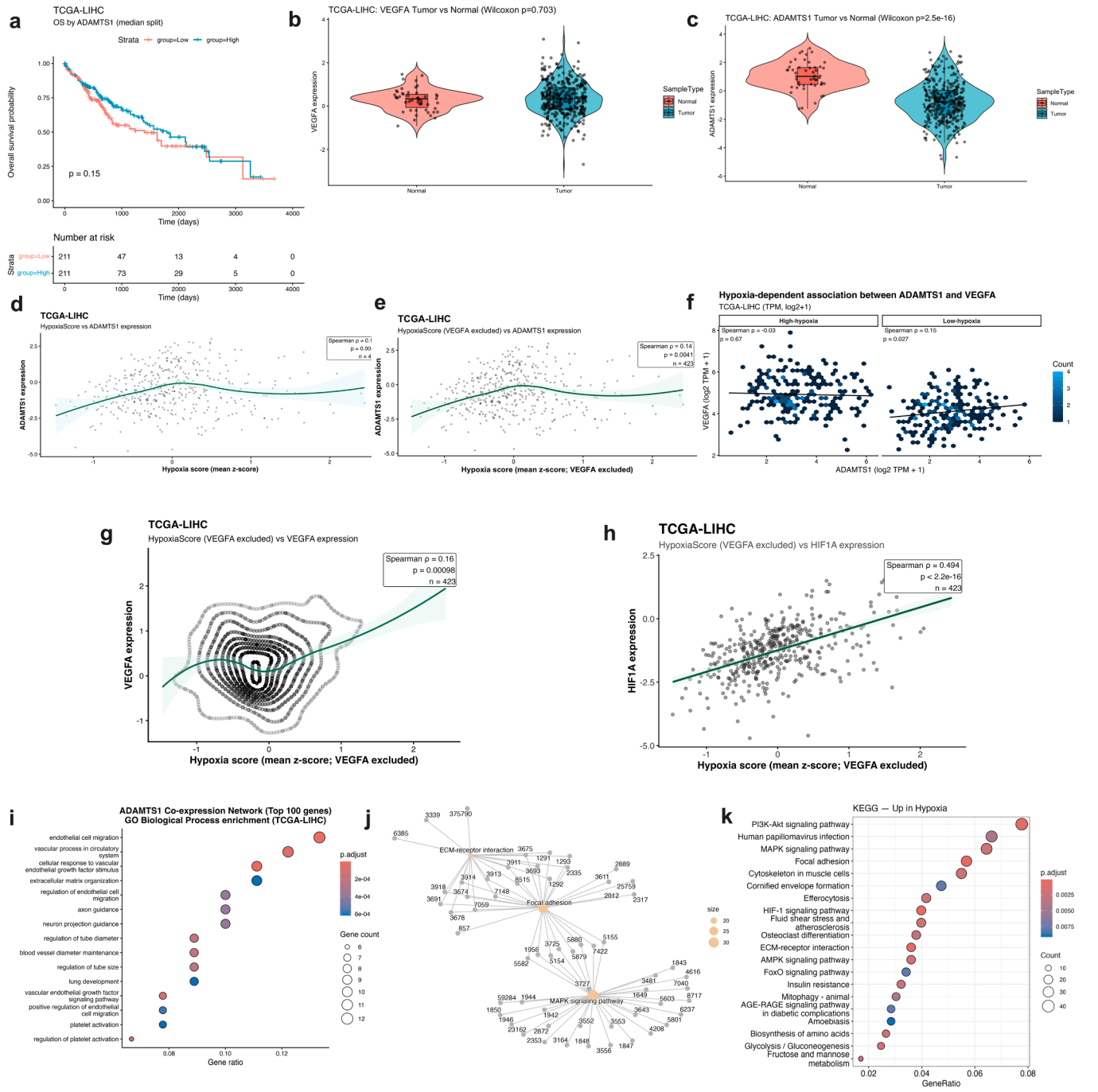


**Fig. 7.** Bioinformatic analyses supporting hypoxia-associated relationships among VEGFA, HIF-1α, and ADAMTS1 in TCGA-LIHC (a) Kaplan–Meier overall survival analysis of TCGA-LIHC patients stratified by ADAMTS1 expression (median split). (b–c) Comparison of VEGFA (b) and ADAMTS1 (c) expression levels between tumor and normal liver tissues in the TCGA-LIHC cohort, shown as violin plots. (d) Association between hypoxia score and ADAMTS1 expression in TCGA-LIHC samples. (e) Association between hypoxia score (calculated excluding VEGFA expression) and ADAMTS1 expression. (f) Hypoxia-dependent association between ADAMTS1 and VEGFA expression in TCGA-LIHC samples, shown separately for low- and high-hypoxia groups. (g) Correlation between hypoxia score (VEGFA excluded) and VEGFA expression in TCGA-LIHC samples. Spearman correlation coefficient (ρ), p value, and sample size (n) are indicated. (h) Correlation between hypoxia score (VEGFA excluded) and HIF1A expression in TCGA-LIHC samples. (i) Gene Ontology (GO) biological process enrichment analysis of genes co-expressed with ADAMTS1 in TCGA-LIHC. (j) Network visualization of ADAMTS1 co-expressed genes (top 100) in the TCGA-LIHC cohort. (k) KEGG pathway enrichment analysis of hypoxia-upregulated genes in TCGA-LIHC samples. All analyses were performed using TCGA-LIHC transcriptomic data. Correlation analyses were conducted using Spearman's rank correlation test. Enrichment analyses were adjusted for multiple testing where applicable.

participate in coordinated, hypoxia-associated transcriptional relationships in hepatocellular carcinoma. While these findings remain correlative, they provide clinically relevant support for the oxygen-sensitive regulatory interactions suggested by the *in vitro* data.

## 4. Discussion

ADAMTS1 is a secretory metalloproteinase that plays a role in the dynamic reorganization of the extracellular matrix. The effects of ADAMTS1 on cancer vary depending on the context and tumor type;

some studies have reported tumor progression promotion, while others have reported tumor-suppressive effects (de Arao Tan et al., 2013). Studies specifically conducted on HCC have reported lower ADAMTS1 expression than that in intact liver tissue. This reduced expression suggests that it may predispose patients to HCC development through liver fibrogenesis and microenvironmental remodeling processes rather than through direct tumor effects. ADAMTS1 is a potent anti-angiogenic agent. It performs this function by directly binding and sequestering the $VEGFA_{165}$ isoform, specifically via its C-terminal domain, thereby preventing VEGFA from accessing its receptors and restricting endothelial cell proliferation and neovascularization (Kumar et al., 2012). This mechanism is consistent with the observation of a negative correlation between ADAMTS1 and VEGFA expression in hepatocellular tumors. However, the decreased expression of ADAMTS1 in invasive HCC specimens and the potential for the complete form of the protease or its proteolytic fragments to exert pro- or anti-metastatic effects in different contexts suggest that the role of ADAMTS1 in HCC pathogenesis is complex and context-dependent. These contradictory biological effects should be carefully examined, particularly considering ECM components, signaling pathways, and cell type-dependent microenvironmental conditions. Based on these studies, it is of interest to investigate changes in ADAMTS1 gene expression in the presence of VEGFA cytokine in hepatocellular carcinoma under hypoxic and normoxic conditions.

A comparison of ADAMTS1 mRNA levels in Hep3B and Saos-2 cells reveal the differential basal expression in both cell lines. It has been previously reported that ADAMTS1 is expressed at different levels depending on the tumor type, playing a tumor-suppressive role in HCC and a regulatory role in matrix remodeling in osteosarcoma (de Assis Lima et al., 2021; Théret, Bouezzeddine, et al., 2021). This difference indicates that ADAMTS1 is transcriptionally regulated in a cell type-and microenvironmental condition-sensitive manner. In addition, we demonstrated that VEGFA increases ADAMTS1 expression under both normoxic and hypoxic conditions; however, the timing of this induction varies depending on the oxygen levels. These different kinetic responses indicate that ADAMTS1 transcription is dynamically regulated by the interaction between VEGFA signaling and hypoxia-responsive transcription factors. The literature indicates that ADAMTS1 is a metalloprotease that regulates VEGFA bioavailability in angiogenesis and the tumor microenvironment (Luque et al., 2003b; Rodríguez-Manzaneque et al., 2015). Interestingly, the increase in ADAMTS1 observed in the early stages under hypoxic conditions is likely due to HIF-1α-mediated transcriptional activation (Hatipoglu et al., 2009), but decreases in subsequent hours due to HIF-dependent feedback inhibitory mechanisms (e.g., BACH1 or DEC1) (Kitamuro et al., 2003; MA et al., 2013). In contrast, the increase in ADAMTS1 in the late stage under normoxic conditions is likely related to VEGFA-mediated ERK/Akt signaling and SP1-mediated transcriptional activation (Wang et al., 2019).

At the cellular level, VEGFA stimulation upregulated ADAMTS1 transcription and protein expression in Hep3B cells, with a stronger and earlier response observed in hypoxia. This regulation is mediated primarily through multiple signal transduction pathways, as shown by inhibitor studies. Simultaneously, the transcriptional and post-transcriptional regulatory effects of VEGFA on ADAMTS1 expression were evaluated under normoxic and hypoxic conditions. Luciferase reporter gene assays performed under hypoxic conditions revealed a significant increase in luciferase activity with VEGFA application in the P7 construct, and this increase was significantly reduced in the presence of the MEK/ERK inhibitor PD98059 (PD9). This finding indicates that VEGFA activates the ADAMTS1 promoter via the MEK/ERK pathway under hypoxic conditions. Western blot analyses correlated with these findings, confirming that VEGFA increases ADAMTS1 protein expression in a hypoxic environment and that this effect is reduced in the presence of PD98059.

In this study, we demonstrate that ADAMTS1 transcriptional regulation is oxygen-sensitive and that, under hypoxic conditions, VEGFA-triggered intracellular signaling networks converge on the ADAMTS1 promoter through multiple transcription factor (TF) modules. ChIP–qPCR validation of *in silico*–identified ELK1, c-JUN, and ATF-1 motifs indicates that the ADAMTS1 promoter is not governed by a classical "single TF–single pathway" mechanism, but rather by signal convergence of parallel cascades such as MAPK and PI3K at the same promoter region. Our ELK1-related findings support the involvement of a TCF (ternary complex factor) module linked to the ERK/p38/JNK axis at the ADAMTS1 promoter. ERK1/2-dependent phosphorylation of ELK-1 and its role in enhancing transcriptional activity and ternary complex formation are well established (Gille et al., 1995). Moreover, both p38 and JNK have been shown to contribute to ELK-1/TCF activation (Whitmarsh et al., 1997). In this context, the differential ELK1 enrichment patterns observed between normoxic and hypoxic conditions suggest that oxygen availability can reprogram MAPK-dependent TCF dynamics at the ADAMTS1 promoter.

Similarly, our c-JUN (AP-1) binding data are consistent with reports showing that hypoxia activates the AP-1 axis, thereby modulating promoter binding and transcriptional output. In hypoxic HepG2 cells, AP-1 activation has been linked to JNK signaling and c-Jun phosphorylation, with functional AP-1 binding sites playing a critical regulatory role (Minet et al., 2001). The detection of c-JUN binding under both oxygen conditions, coupled with region-specific enrichment differences, supports the notion that the ADAMTS1 promoter exhibits basal AP-1 accessibility that is selectively reinforced through stress-responsive MAPK signaling under hypoxia.

One of the most prominent findings of this study is the marked and widespread increase in ATF-1 promoter occupancy under hypoxic conditions. ATF-1 transcriptional activity is known to be enhanced by phosphorylation, particularly at Ser63, which increases DNA binding and transcriptional output (Kobayashi et al., 1997). ERK-mediated downstream kinase signaling has also been shown to phosphorylate ATF-1 in a manner required for target gene expression (Gupta & Prywes, 2002). In addition, the nuclear kinase MSK1—activated by ERK and p38—has been identified as a key mediator of CREB/ATF-1 phosphorylation in mitogenic and stress responses (Deak et al., 1998). Accordingly, the enhanced recruitment of ATF-1 to the ADAMTS1 promoter under hypoxia likely reflects functional reprogramming driven by stress-activated MAPK nodes (p38/JNK/ERK) rather than a simple increase in TF abundance.

The data obtained in this study show that VEGFA positively regulates its own expression and HIF-1α levels under both normoxic and hypoxic conditions. This result is consistent with previous studies showing that VEGFA enhances its own promoter activity through a feedback mechanism (Forsythe et al., 1996). This autoinduction effect of VEGFA emerged earlier and more strongly under hypoxic conditions, suggesting that hypoxia-related transcription factors (particularly HIF-1α) facilitate this process. The marked increase observed in HIF-1α levels reached a maximum at 24–48 h following VEGFA administration, both at the mRNA and protein levels. This finding has been interpreted as VEGFA inducing HIF-1α transcription and simultaneously increasing HIF-1α protein stability. This finding demonstrates that VEGFA is not only a downstream target of HIF-1α but also functions as an upstream regulator of HIF-1α. Indeed, a bidirectional feedback loop between VEGFA and HIF-1α has been previously reported, particularly supporting hypoxic adaptation, angiogenesis, and cell survival in tumor cells (Liu et al., 1995). This reciprocal interaction demonstrates that VEGFA plays a role not only as a vascular endothelial growth factor in the hypoxic microenvironment but also as an HIF-1α -mediated transcriptional activator. By increasing its own expression, VEGFA enhances the cells' capacity to adapt to oxygen deprivation while supporting processes such as angiogenesis, metabolic reprogramming, and cell migration through the stabilization of HIF-1α (Pagès & Pouysségur, 2005). In summary, these findings demonstrate that the VEGFA- HIF-1α axis forms a bidirectional positive feedback mechanism and that this interaction constitutes a fundamental molecular circuit that sustains angiogenesis and tumor progression, particularly in the hypoxic tumor microenvironment. The

bioinformatic analyses of GEO-derived transcriptomic data further substantiated this connection, revealing coordinated upregulation of ADAMTS1, VEGFA, and HIF-1α and enrichment of the HIF1-α, PI3K–Akt, and ECM–receptor interaction pathways in hypoxia.

Taken together, our findings indicate that ADAMTS1 is linked to hypoxia-associated angiogenic regulation in the tumor microenvironment. Nevertheless, the present results are based on correlative evidence, and a direct functional role of ADAMTS1 in VEGFA-mediated hypoxic responses cannot be inferred at this stage. Further studies employing loss-of-function approaches will be required to clarify the contribution of ADAMTS1 to hypoxia-driven angiogenic processes.

## CRediT authorship contribution statement

**Feray Kockar:** Writing – original draft, Visualization, Validation, Supervision, Software, Methodology, Investigation, Formal analysis, Project administration. **Esra Tokay:** Writing – original draft, Visualization, Validation, Supervision, Software, Methodology, Investigation, Formal analysis. **Nelin Hacioglu:** Writing – original draft, Visualization, Validation, Supervision, Software, Methodology, Investigation, formal analysis. **Yasemin Kalfa:** Methodology, Formal analysis. **Kubilay Gunerhan:** Methodology, Formal analysis. **Merve Karaman:** Methodology, Formal analysis. **Feyza Nur Sav:** Methodology, Formal analysis. **Kubra Zehra Kalay:** Methodology, Formal analysis. **Meltem Balaban:** Methodology, Formal analysis.

## Ethics approval

This study did not involve animals or humans, and therefore, ethical approval was not required.

## Funding

This study was financially supported by The Scientific and Technological Research Council of Türkiye (TÜBİTAK), Grant No: 110T961.

## Declaration of Competing Interest

The authors declare no relevant financial or non-financial interests.

## Appendix A. Supporting information

Supplementary data associated with this article can be found in the online version at doi:10.1016/j.tice.2026.103395.

## Data availability

Data will be made available on request.

## References

Ahlquist, T., Lind, G.E., Costa, V.L., Meling, G.I., Vatn, M., Hoff, G.S., Rognum, T.O., Skotheim, R.I., Thiis-Evensen, E., Lothe, R.A., 2008. Gene methylation profiles of normal mucosa, and benign and malignant colorectal tumors identify early onset markers. Mol. Cancer 7, 94. https://doi.org/10.1186/1476-4598-7-94.

Alper, M., Kockar, F., 2014. IL-6 upregulates a disintegrin and metalloproteinase with thrombospondin motifs 2 (ADAMTS-2) in human osteosarcoma cells mediated by JNK pathway. Mol. Cell. Biochem. 393 (1–2), 165–175. https://doi.org/10.1007/s11010-014-2056-9.

Alper, M., Sav, F.N., Keleş, Y., Eroğlu, K.P., Keskin, S.D., Köçkar, F., 2025. STAT-3, ELK-1, and c- Jun contributes IL-6 mediated ADAMTS-8 upregulation in colorectal cancer. Mol. Biol. Rep. 52 (1), 246. https://doi.org/10.1007/s11033-025-10342-4.

Altuntaş, C., Alper, M., Keleş, Y., Sav, F.N., Köçkar, F., 2023a. Hypoxic regulation of ADAMTS-2 and -3 (a disintegrin and matrix metalloproteinase with thrombospondin motifs 2 and 3) procollagen N proteinases by HIF-1α in endothelial cells. Mol. Cell. Biochem. 478 (5), 1151–1160. https://doi.org/10.1007/S11010-022-04549-3.

Bakleh, M.Z., Al Haj Zen, A., 2025. The distinct role of HIF-1α and HIF-2α in hypoxia and angiogenesis. Cells 14 (9). https://doi.org/10.3390/cells14090673.

Brogowska, K.K., Zajkowska, M., Mroczko, B., 2023. Vascular endothelial growth factor ligands and receptors in breast cancer. J. Clin. Med. 12 (6). https://doi.org/10.3390/jcm12062412.

Byrne, A.M., Bouchier-Hayes, D.J., Harmey, J.H., 2005. Angiogenic and cell survival functions of vascular endothelial growth factor (VEGF). J. Cell. Mol. Med. 9 (4), 777–794. https://doi.org/10.1111/j.1582-4934.2005.tb00379.x.

Castro-Rivera, E., Ran, S., Brekken, R.A., Minna, J.D., 2008. Semaphorin 3B inhibits the phosphatidylinositol 3-kinase/Akt pathway through neuropilin-1 in lung and breast cancer cells. Cancer Res. 68 (20), 8295–8303. https://doi.org/10.1158/0008-5472.CAN-07-6601.

Chen, Y., Liu, Y., Zhou, J., Bao, T., Wang, J., Ao, M., 2025. Adamantyl-substituted chalcone CA13 induces cytoprotective autophagy and JNK-dependent apoptosis in lung cancer cells. Biomolecules 16 (1), 54. https://doi.org/10.3390/biom16010054.

Chou, C.-W., Chen, C.-C., 2008. HDAC inhibition upregulates the expression of angiostatic ADAMTS1. FEBS Lett. 582 (29), 4059–4065. https://doi.org/10.1016/j.febslet.2008.10.048.

de Arao Tan, I., Ricciardelli, C., Russell, D.L., 2013. The metalloproteinase ADAMTS1: a comprehensive review of its role in tumorigenic and metastatic pathways. Int. J. Cancer 133 (10), 2263–2276. https://doi.org/10.1002/ijc.28127.

de Assis Lima, M., da Silva, S.V., Serrano-Garrido, O., Hülsemann, M., Santos-Neres, L., Rodríguez-Manzaneque, J.C., Hodgson, L., Freitas, V.M., 2021. Metalloprotease ADAMTS-1 decreases cell migration and invasion modulating the spatiotemporal dynamics of Cdc42 activity. Cell. Signal. 77, 109827. https://doi.org/10.1016/j.cellsig.2020.109827.

Ferrara, N., 2001. Role of vascular endothelial growth factor in regulation of physiological angiogenesis. Am. J. Physiol. Cell Physiol. 280 (6), C1358–C1366. https://doi.org/10.1152/ajpcell.2001.280.6.C1358.

Fontanini, G., Lucchi, M., Vignati, S., Mussi, A., Ciardiello, F., De Laurentiis, M., De Placido, S., Basolo, F., Angeletti, C.A., Bevilacqua, G., 1997. Angiogenesis as a prognostic indicator of survival in non-small-cell lung carcinoma: a prospective study. J. Natl. Cancer Inst. 89 (12), 881–886. https://doi.org/10.1093/jnci/89.12.881.

Forsythe, J.A., Jiang, B.H., Iyer, N.V., Agani, F., Leung, S.W., Koos, R.D., Semenza, G.L., 1996. Activation of vascular endothelial growth factor gene transcription by hypoxia-inducible factor 1. Mol. Cell. Biol. 16 (9), 4604–4613. https://doi.org/10.1128/MCB.16.9.4604.

Gille, H., Kortenjann, M., Thomae, O., Moomaw, C., Slaughter, C., Cobb, M.H., Shaw, P.E., 1995. ERK phosphorylation potentiates Elk-1-mediated ternary complex formation and transactivation. EMBO J. 14 (5), 951–962. https://doi.org/10.1002/J.1460-2075.1995.TB07076.X/METRICS.

Gungor, T., Yetis, G., Onder, F.C., Tokay, E., Tok, T.T., Celik, A., Ay, M., Kockar, F., 2018. Prodrugs for nitroreductase based cancer therapy- 1: metabolite profile, cell cytotoxicity and molecular modeling interactions of nitro benzamides with Ssap-NtrB. Med. Chem. 14 (5), 495–507. https://doi.org/10.2174/1573406413666171129224424.

Gustavsson, H., Jennbacken, K., Welén, K., Damber, J.-E., 2008. Altered expression of genes regulating angiogenesis in experimental androgen-independent prostate cancer. Prostate 68 (2), 161–170. https://doi.org/10.1002/pros.20672.

Hatipoglu, O.F., Hirohata, S., Cilkek, M.Z., Ogawa, H., Miyoshi, T., Obika, M., Demircan, K., Shihohata, R., Kusachi, S., Ninomiya, Y., 2009. ADAMTS1 is a unique hypoxic early response gene expressed by endothelial cells. J. Biol. Chem. 284 (24), 16325–16333. https://doi.org/10.1074/jbc.M109.001313.

Hu, X., Li, J., Fu, M., Zhao, X., Wang, W., 2021. The JAK/STAT signaling pathway: from bench to clinic. Signal Transduct. Target. Ther. 6 (1), 402. https://doi.org/10.1038/s41392-021-00791-1.

Kitamuro, T., Takahashi, K., Ogawa, K., Udono-Fujimori, R., Takeda, K., Furuyama, K., Nakayama, M., Sun, J., Fujita, H., Hida, W., Hattori, T., Shirato, K., Igarashi, K., Shibahara, S., 2003. Bach1 functions as a hypoxia-inducible repressor for the heme oxygenase-1 gene in human cells. J. Biol. Chem. 278 (11), 9125–9133. https://doi.org/10.1074/jbc.M209939200.

Kumar, S., Rao, N., Ge, R., 2012. Emerging roles of ADAMTSs in angiogenesis and cancer. Cancers 4 (4), 1252–1299. https://doi.org/10.3390/cancers4041252.

Kuno, K., Kanada, N., Nakashima, E., Fujiki, F., Ichimura, F., Matsushima, K., 1997. Molecular cloning of a gene encoding a new type of metalloproteinase-disintegrin family protein with thrombospondin motifs as an inflammation associated gene. J. Biol. Chem. 272 (1), 556–562. https://doi.org/10.1074/jbc.272.1.556.

Liu, Y., Cox, S.R., Morita, T., Kourembanas, S., 1995. Hypoxia regulates vascular endothelial growth factor gene expression in endothelial cells. Identif. a 5' Enhanc. Circ. Res. 77 (3), 638–643. https://doi.org/10.1161/01.res.77.3.638.

Livak, K.J., Schmittgen, T.D., 2001. Analysis of relative gene expression data using real-time quantitative PCR and the 2-ΔΔCT method. Methods 25 (4), 402–408. https://doi.org/10.1006/meth.2001.1262.

Lugano, R., Ramachandran, M., Dimberg, A., 2020. Tumor angiogenesis: causes, consequences, challenges and opportunities. Cell. Mol. Life Sci. CMLS 77 (9), 1745–1770. https://doi.org/10.1007/s00018-019-03351-7.

MA, W., SHI, X., LU, S., WU, L., WANG, Y., 2013. Hypoxia-induced overexpression of DEC1 is regulated by HIF-1α in hepatocellular carcinoma. Oncol. Rep. 30 (6), 2957–2962. https://doi.org/10.3892/or.2013.2774.

Minet, E., Michel, G., Mottet, D., Piret, J.P., Barbieux, A., Raes, M., Michiels, C., 2001. c-JUN gene induction and AP-1 activity is regulated by a JNK-dependent pathway in hypoxic HepG2 cells. Exp. Cell Res. 265 (1), 114–124. https://doi.org/10.1006/excr.2001.5180.

Nelson, J.D., 2006. Fast chromatin immunoprecipitation assay. Nucleic Acids Res. 34 (1). https://doi.org/10.1093/nar/gnj004 e2–e2.

Pagès, G., Pouysségur, J., 2005. Transcriptional regulation of the Vascular Endothelial Growth Factor gene–a concert of activating factors. Cardiovasc. Res. 65 (3), 564–573. https://doi.org/10.1016/j.cardiores.2004.09.032.

Porter, S., Clark, I.M., Kevorkian, L., Edwards, D.R., 2005. The ADAMTS metalloproteinases. Biochem. J. 386 (Pt 1), 15–27. https://doi.org/10.1042/BJ20040424.

Rocks, N., Paulissen, G., El Hour, M., Quesada, F., Crahay, C., Gueders, M., Foidart, J.M., Noel, A., Cataldo, D., 2008. Emerging roles of ADAM and ADAMTS metalloproteinases in cancer. Biochimie 90 (2), 369–379. https://doi.org/10.1016/j.biochi.2007.08.008.

Rodríguez-Manzaneque, J.C., Fernández-Rodríguez, R., Rodríguez-Baena, F.J., Iruela-Arispe, M.L., 2015. ADAMTS proteases in vascular biology. Matrix Biol. 38–45. https://doi.org/10.1016/j.matbio.2015.02.004.

Senger, D.R., Galli, S.J., Dvorak, A.M., Perruzzi, C.A., Harvey, V.S., Dvorak, H.F., 1983. Tumor cells secrete a vascular permeability factor that promotes accumulation of ascites fluid. Science 219 (4587), 983–985. https://doi.org/10.1126/science.6823562.

Srivastava, A., Laidler, P., Davies, R.P., Horgan, K., Hughes, L.E., 1988. The prognostic significance of tumor vascularity in intermediate-thickness (0.76–4.0 mm thick) skin melanoma. A quantitative histologic study. Am. J. Pathol. 133 (2), 419–423.

Tang, B.L., 2001. ADAMTS: a novel family of extracellular matrix proteases. Int. J. Biochem. Cell Biol. 33 (1), 33–44. https://doi.org/10.1016/S1357-2725(00)00061-3.

Théret, N., Bouezzeddine, F., Azar, F., Diab-Assaf, M., Legagneux, V., 2021. ADAM and ADAMTS proteins, new players in the regulation of hepatocellular carcinoma microenvironment. Cancers 13 (7), 1563. https://doi.org/10.3390/cancers13071563.

Tokay, E., Kockar, F., 2016a. Identification of intracellular pathways through which TGF-β1 upregulates URG-4/URGCP gene expression in hepatoma cells. Life Sci. 144, 121–128. https://doi.org/10.1016/j.lfs.2015.12.010.

Tokay, E., Kockar, F., 2016b. SP1 is a transcriptional regulator of URG-4/URGCP gene in hepatocytes. Mol. Cell. Biochem. 423 (1–2), 75–83. https://doi.org/10.1007/s11010-016-2826-7.

Turkoglu, S.A., Kockar, F., 2016. SP1 and USF differentially regulate ADAMTS1 gene expression under normoxic and hypoxic conditions in hepatoma cells. Gene 575 (1), 48–57. https://doi.org/10.1016/j.gene.2015.08.035.

Vázquez, F., Hastings, G., Ortega, M.A., Lane, T.F., Oikemus, S., Lombardo, M., Iruela-Arispe, M.L., 1999. METH-1, a human ortholog of ADAMTS-1, and METH-2 are members of a new family of proteins with angio-inhibitory activity. J. Biol. Chem. 274 (33), 23349–23357. https://doi.org/10.1074/jbc.274.33.23349.

Veikkola, T., Karkkainen, M., Claesson-Welsh, L., Alitalo, K., 2000. Regulation of angiogenesis via vascular endothelial growth factor receptors. Cancer Res. 60 (2), 203–212.

Vempati, P., Popel, A.S., Mac Gabhann, F., 2014. Extracellular regulation of VEGF: isoforms, proteolysis, and vascular patterning. Cytokine Growth Factor Rev. 25 (1), 1–19. https://doi.org/10.1016/j.cytogfr.2013.11.002.

Wang, B., Chen, S., Zhao, J.-Q., Xiang, B.-L., Gu, X., Zou, F., Zhang, Z.-H., 2019. ADAMTS-1 inhibits angiogenesis via the PI3K/Akt-eNOS-VEGF pathway in lung cancer cells. Transl. Cancer Res. 8 (8), 2725–2735. https://doi.org/10.21037/tcr.2019.10.34.

Whitmarsh, A.J., Yang, S.-H., Su, M.S.-S., Sharrocks, A.D., Davis, R.J., 1997. Role of p38 and JNK mitogen-activated protein kinases in the activation of ternary complex factors. Mol. Cell. Biol. 17 (5), 2360–2371. https://doi.org/10.1128/MCB.17.5.2360.